Use of impulses to determine the reaction force of a hydraulic structure with an overhang due to wave impact

Chen, Xuexue; Hofland, Bas; Molenaar, Wilfred; Capel, Alex; Van Gent, Marcel R.A.

DOI
10.1016/j.coastaleng.2019.02.003

Publication date
2019

Document Version
Accepted author manuscript

Published in
Coastal Engineering

Use of impulses to determine the reaction force of hydraulic structure with an overhang due to wave impact

Xuexue Chen[a,c], Bas Hofland[a,b], Wilfred Molenaar[a], Alex Capel[b], Marcel R.A. Van Gent[b]

[a] *Dept.of Hydraulic Eng., Delft University of Technology, Stevinweg 1, 2628 CN Delft, The Netherlands*
[b] *Dept.of Coastal Structures and Waves, Deltares, PO Box 177, 2600 MH Delft, The Netherlands*
[c] *Royal HaskoningDHV, George Hintzenweg 85, 3009 AM Rotterdam, The Netherlands*

Abstract

This paper describes a method of determining the reaction forces of a vertical structure with an overhang to impulsive wave impacts. The aim is to develop a method to design a hydraulic structure exposed to the impulsive wave impact. At present, there is a lack of guidelines on the designing and verification with such a purpose. The impulse of the impact is taken as the primary design variable to estimate the impulsive reaction force instead of peak impact forces. By using extreme value analysis (EVA), the characteristic impulse (e.g., $I_{im,0.1\%}$) can be determined. Then a simple structure model is used for obtaining reaction forces to the characteristic impact impulse. The sum of the impulsive reaction force and the quasi-steady wave force could represent the total reaction force, which can be used as a design load on the structure. The advantage of using the impact impulse could give an approach in which several aspects of the impulsive wave impact force can be incorporated better, like determining the exceedance probability of a certain load, incorporating the flexibility of the structure and correcting possible scale effects in small scale hydraulic models. The proposed method based on the characteristic value of the $I_{im,0.1\%}$ is applied to forces measured in a small scale model of the Afsluitdijk discharge sluice, and compared well to a full time domain solution. The results indicate the initial assumption that using the impact impulse of the impact as the primary design variable, it is possible to estimate the dynamic response of the structure.

Keywords: Wave impact; Dynamic response; Impact impulse; Vertical structure with an overhang

1. Introduction

Waves can give intensive impacts with very short duration. In the design of marine structures, this type of impulsive impact is a primary concern, but it is seldom regarded explicitly in the structural analysis of hydraulic structures or in an overly simplified manner. This conventional approval of exclusion is due to

*Corresponding author
Email address: Xuexue.Chen@rhdhv.com (Xuexue Chen)

the low natural frequencies (or long natural vibration period) of the entire structure compared to the very short wave impact duration.

Many hydraulic structures like sluice gates, lock gates, and storm surge barriers often contain slender features like steel gates (e.g., Eastern Scheldt storm surge barrier and Afsluitdijk discharge sluices in the Netherlands and Thames barrier in the UK), which may have a complicated dynamic behavior under impulsive wave impact forces. Meanwhile, many of these existing large hydraulic structures are coming close to the end of their envisaged lifetime, such that new structures and temporary maintenance structures have to be designed. The need has arisen for a simple and quick means of estimating reaction forces for structural engineers. In many cases, it is not clear whether the impulsive force on the structure or structural components will be damped or amplified dynamically.

The qualitative and quantitative experimental determination of the impulsive wave impact forces on vertical structures has been examined widely in the past decades (e.g., Bagnold, 1939; Nagai, 1973; Ramkema, 1978; Chan and Melville, 1988; Oumeraci et al., 1993; Bullock et al., 2001; Cuomo et al., 2010a) and walls with overhang (e.g., Kisacik et al., 2012), recurved parapets (e.g., Castellino et al., 2018) and inclined walls (e.g., Losada et al., 1995). These studies have demonstrated that wave impulsive forces on walls can be much higher than quasi-steady forces (or pulsating forces) predicted by standard methods and involve complex impact mechanisms, such as flip-through and breaking wave impact. The term quasi-steady force means the wave force is caused by slowly varied water motion, which can be dealt with relatively straightforward, for instance by using the theory of Sainflou (1928) for regular, non-breaking standing waves. The current manuals and well-known design methods are often too simplified for the wave impact force. These simplifications lead to conservative designs and constructions. Sometimes a measured peak-force is taken such that it is too conservative, or sometimes it is just said that impacts should be avoided. There are few design methods of wave impact forces intended for hydraulic structures. This lack of knowledge became clear during projects like the design of the gates of the discharges sluices, grid beams of storm surge barriers (see Fig. 1). For this situation, scaled physical or numerical model tests are commonly used to determine the impulsive wave force. Then the obtained forces are used for the design impact load. However, it is still unclear how to deal with these measured or calculated short-duration impulsive forces from scaled model tests. Not using these forces might underestimate the design reaction force, but using these forces could lead to a vast overestimation of the design load. Kirkgoz and Mengi (1986) and Takahashi et al. (1998) took dynamic response analysis of cassion walls against wave impact to obtain reaction forces. However, the analysis was limited to the cassion type vertical structures. Other hydraulic structures containing slender features like steel gates and more complex geometrical structures like vertical wall with overhangs were not considered.

At present no method exists in which the impulsive load is described in a physically realistic and statistically sound way, such that it can be used to calculate the dynamic response of these structures. In this paper, a first attempt is made to formulate a design method based on splitting the impulsive part of the

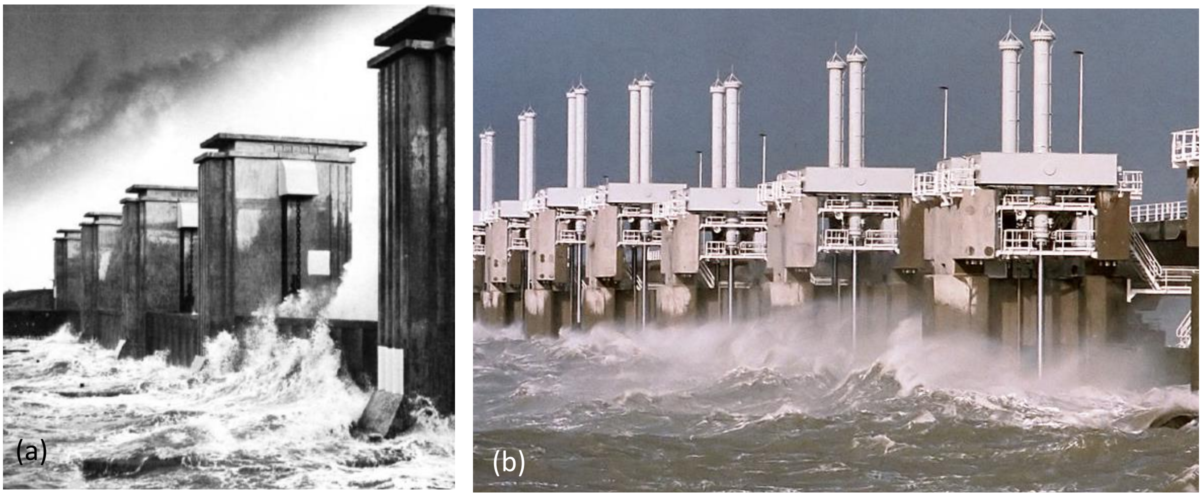

Fig. 1: (a) Wave impacts on the defence beams of the old sluice gates of Afsluitdijk; (b) wave impacts on the Oosterschelde barrier (Rijkswaterstaat).

wave impact load. The novelty of the approach is that the impact impulse of wave impacts will be taken as the primary design variable instead of the peak force or pressure of the impacts. Using the impact impulse could give an approach in which several aspects of wave loads can be incorporated better, like determining the exceedance probability of a certain load, incorporating the flexibility of the structure, correcting possible scale effects in small scale in hydraulic models, and determining the spatial distribution of the wave loads.

This paper is structured as follows. In Chapter 2, a brief introduction of wave impact and wave impact as a loading are given. Then, in Chapter 3 the envisaged design approach is described, in which small scale model results can be translated to flexible prototype structures. In Chapter 4, a description of analyzed physical model tests is given. In Chapter 5, experimental observations, and evaluation of the proposed envisaged design approach by using the measured wave forces are given. Finally, a short discussion and conclusion are presented in Chapter 6 and 7.

2. Wave impact and impact loading

2.1. Wave impact

A typical time series of wave impact force consists of two components: one is the impulsive force F_{im}, which changes with time quickly; the other is the quasi-steady force F_{qs+}, which varies very slowly, as shown in Fig. 2. The shaded area in the figure, the impact impulse (I_{im}), is defined as the time integral of the impulsive force over the impact duration T_d. It is the impulsive part of the impacts, the high frequency part of the load that is caused by the sudden contact of the water surface with the structure. For an impulsive impact, the duration of the impact T_d can be very short compared to the natural period of the structure, but the force magnitude can be even more than 10 times its quasi-steady force. Impulsive wave impacts can also be expected when the wave is confined at corners between walls and overhanging type structures (e.g., horizontal decks and beams), and by the influences of the air (e.g., Ramkema, 1978). For these cases, recently an analytical solution to determine the pressure impulse has been formulated (e.g., Wood and Peregrine, 1997; Md Noar, 2012; Md Noar and Greenhow, 2015). A brief introduction and the application of using the pressure-impulse are presented in Appendix A.

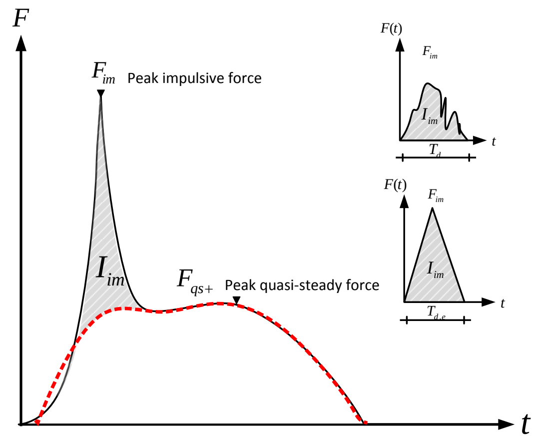

Fig. 2: Typical time history of a wave impact on a (vertical) wall with or without a horizontal overhang, I_{im} denotes the impact impulse

.

The peak-forces of the impulsive impacts on a vertical wall exhibit a large variation among the existing reported laboratory measurements since Bagnold (1939). This variation is partly contributed by scale and model effects. But apart from these influences, the nature of impact loads is also very variable. It is observed that identical waves can give variable impact force peaks on the same structure (Bagnold, 1939; Losada et al., 1995; Hofland et al., 2010). Therefore, it is hard to accurately predict the peak value of the impulsive impact.

It has been recognized that impact impulse is more predictable than pressure or force peaks (e.g., Cooker and Peregrine, 1990, 1995; Cuomo et al., 2010b; Hofland et al., 2010). Thus, using impact impulse may result in a simplified but much more stable model of wave impact on the structures. And there is also the possibility of using it to predict the impulse of wave impact forces theoretically, when the velocities are known (e.g., upward velocity of standing waves), or the spatial distribution has to be estimated. These velocities can be better predicted than the wave impact pressures or the impact forces. However, the definition and determination of the impulsive impact component is still not clear.

Table 1: Three loading domains of a structure (Humar, 2002)

Loading domain	T_d/T_n	Reaction force and actual load
Quasi-static	≥ 4	$F_r = F_{max}$
Dynamic	0.25-4	$F_r > F_{max}$
Impulsive	<0.25	$F_r < F_{max}$

2.2. *Wave impact as a loading*

Impact loadings can be divided into three domains according to on the duration of impacts on structures (Humar, 2002). Here impulsive (short), dynamical (medium), and quasi-static (slow) impacts are distinguished (refer to Table 1). These durations are regarded relative to the natural frequency of the structure. In the impulsive domain, the subjected load is over well before the structure reaches its maximum deflection; In this case, the reaction force F_r is less than the measured wave impact force peak F_{max}. In the quasi-static domain, the structure reaches its maximum deflection well before the load is over; In this case, F_r equals almost to F_{max}. But in the dynamic domain, the maximum deflection is reached near the end of the load; In this case, F_r can even become larger than F_{max}.

3. Envisaged design approach

3.1. *Existing approach to determine design reaction force*

To determine the reaction forces 'F_r' of a structure due to dynamic effects, the dynamic response of the structure must be considered. Meanwhile, a statistical description of the characteristic reaction forces is also needed for the structure experiencing an extreme accidental event.

Fig. 3(a) shows a flowchart of the optimal method to determine the characteristic reaction force, $F_{r,0.1\%}$ for instance. The time series of F_r is calculated based on the time series of the wave impact forces obtained from physical model or numerical model tests firstly by using a structural (e.g., finite element) model. Afterwards, $F_{r,0.1\%}$ can be given for example using Extreme Value Analysis (EVA). The drawback of this approach is that obtaining F_r in time domain typically requires too much computational effort.

A simplified approach is widely in use, as shown in Fig. 3(b). A wave impact force peak, F_{max}, by a statistical description is given for example using Extreme Value Analysis (EVA) firstly (e.g., $F_{0.1\%}$), and then the reaction force F_r due to this F_{max} can be estimated by using a structural model to consider the influence of the structural flexibility (e.g., $F_{r,0.1\%}$) or the true record of the maximum force is simply applied to the finite element model. Drawback of this approach is that only the force peaks (F_{max}) are used for statistical analysis. Afterwards, the largest Dynamic Load Factor (DLF) value is used to calculate F_r with the conservative consideration. However, it is still unclear that how to deal with these measured or calculated short-duration impulsive forces from scaled model tests since using these impulsive forces could lead to a vast overestimation of the design load by using DLF.

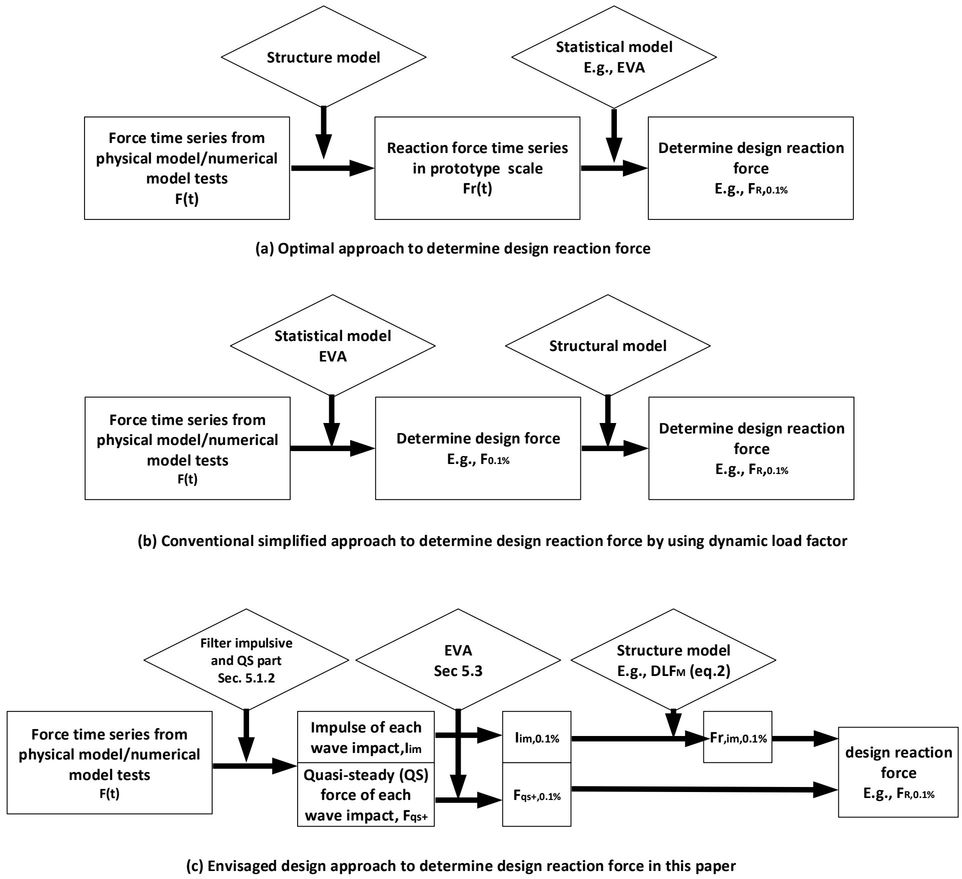

Fig. 3: Three approaches to determine the design reaction forces with a statistical description of the dynamic response of the structure.

3.2. *Envisaged design approach by using impulse as input*

In this study, an envisaged design approach by using the impact impulse I_{im} to estimate the response (e.g., reaction force) of a structure is presented, as shown in Fig. 3(c). The approach consists of an impulse model, a statistical model, and a structural model. The advantage of the proposed approach is to be able to schematize the impacts by using a limited number of parameters such that a statistical description of the force becomes possible. Moreover, scale effects and the flexibility of the structure can be included in a better way. The work flow of the envisaged design approach is described below:

1: Separate the quasi-steady forces from the time series of wave impact forces from scaled model (or CFD model) tests by using a low-pass filter by using the impulse model;

2: After splitting, determine the impact duration T_d of the impulsive component of the impact, the impact impulse I_{im} and quasi steady force F_{qs+};

3: Make Extreme Value Analyses (EVA) of F_{qs+} and I_{im}. Then, determine characteristic value with a certain exceedance probability (e.g., $F_{qs+,0.1\%}$ and $I_{im,0.1\%}$) of these two parts by using the statistical model.

4: The reaction force $F_{im,r,0.1\%}$ of the impulsive component can be calculated based on $I_{im,0.1\%}$ by using the structural model.

5: The design value of the total wave force is re-constructed as $F_{tot,r,0.1\%} = F_{im,r,0.1\%} + F_{qs+,0.1\%}$.

The impulse model, the statistical model, the structural model and the evaluation procedure of the proposed approach are explained in the following sections.

3.3. Impulse model

I_{im} of an impulsive impact is more predictable than force peaks (Bagnold, 1939; Hofland et al., 2010). Thus, using the impact impulse may result in a simplified, but much more stable, model of wave impact on the structures. Based on the pressure-impulse theory (Cooker and Peregrine, 1990, 1995; Wood, 1997), impulsive and quasi-steady components of the wave impact need to be separated. The impact duration might be different in prototype due to scale effects or random variables. An impulse model is developed to split the impulsive and quasi-steady components of the wave impact in order to better predict the impulsive wave impact in the design procedure. The detailed description of using the impulse model for the splitting is given in Section 5.1.2.

3.4. Statistical model

A statistical model is empirically developed based on extreme value analysis of F_{qs+} and I_{im}. Details about this model can be seen in Section 5.3 and Appendix B.

3.5. Structural model

In this paper the authors do not consider the exact structural components of the gate structure. This is part of a different study (Tieleman et al., 2018). The aim is to show that the approach whereby the impulsive is described by a single stochastic variable, could lead to the correct response. To this end the authors assume the gate to be a rigid plate with one degree of freedom: horizontal translation. In the hydraulic model tests the gate was completely rigid. When determining the adequacy of the structure under wave loading, estimating F_r is a simple and direct means in structural design. The ratio between F_r and the force peak F_{max}, called dynamic load factor (DLF) or dynamic amplification factor, is expressed as Eq. 1:

$$\frac{F_r}{F_{max}} = \mathrm{DLF} = f(\frac{T_d}{T_n}). \tag{1}$$

The value of DLF can be determined from a response spectrum as a design chart for the simplified load, and the expression of DLF can be referred to USACE (1957). Thus, when a static response of the structure (e.g. F_{max}) is given, the dynamic response of the structure (e.g. F_r) can be estimated by reading the value of DLF from the response spectrum for an appropriate frequency. In order to simplify the problem, a given structure is replaced by a dynamically equivalent system, herein a linear single degree of freedom model (SDOF) is applied. Fig. 4a shows an example of a dynamic response spectrum for the SDOF system subject to a triangular pulse with different rising time ratio α. The rising time ratio is defined as the ratio between rising time T_r and the total impact duration T_d of the triangular impulse.

In this study, using impulse as the input variable I_{im} to calculate the dynamic response. A modified DLF by using impulse to plot the response spectrum instead of using force peak F_{max} is proposed. In this model, the response function is reformulated and related to the impact impulse, as shown in Eq. 2:

$$\frac{F_r}{I_{im} \cdot \omega_n} = \mathrm{DLF_M} = f(\frac{T_d}{T_n}). \tag{2}$$

Fig 4b gives an example of such a response spectrum which can be used as the design chart. It can be seen that in the impulsive domain ($T_d/T_n < 0.25$) the F_r depends on the impact impulse with a value 1 and it does not depend on the duration (or shape) of the force peak. This is an advantage of using impact impulse to express the response function, as within the impulsive domain the impact duration is difficult to predict. Fig 4b is similar to the fig.5.27 (USACE, 1957) which is used to design structures to against the effects of atomic weapons.

3.6. Evaluation of the envisaged design approach

In order to evaluate this design approach, the research is conduced in four steps: using physical model tests to collect wave impact forces as input; obtaining the total reaction force of the considered structure by using the proposed envisaged design method; using the SDOF model to get total reaction forces due to the time series of the wave impact force as the real structural response; then comparing the total reaction forces from the proposed method with the total reaction forces from the SDOF model. These steps are further specified in Chapter 5.

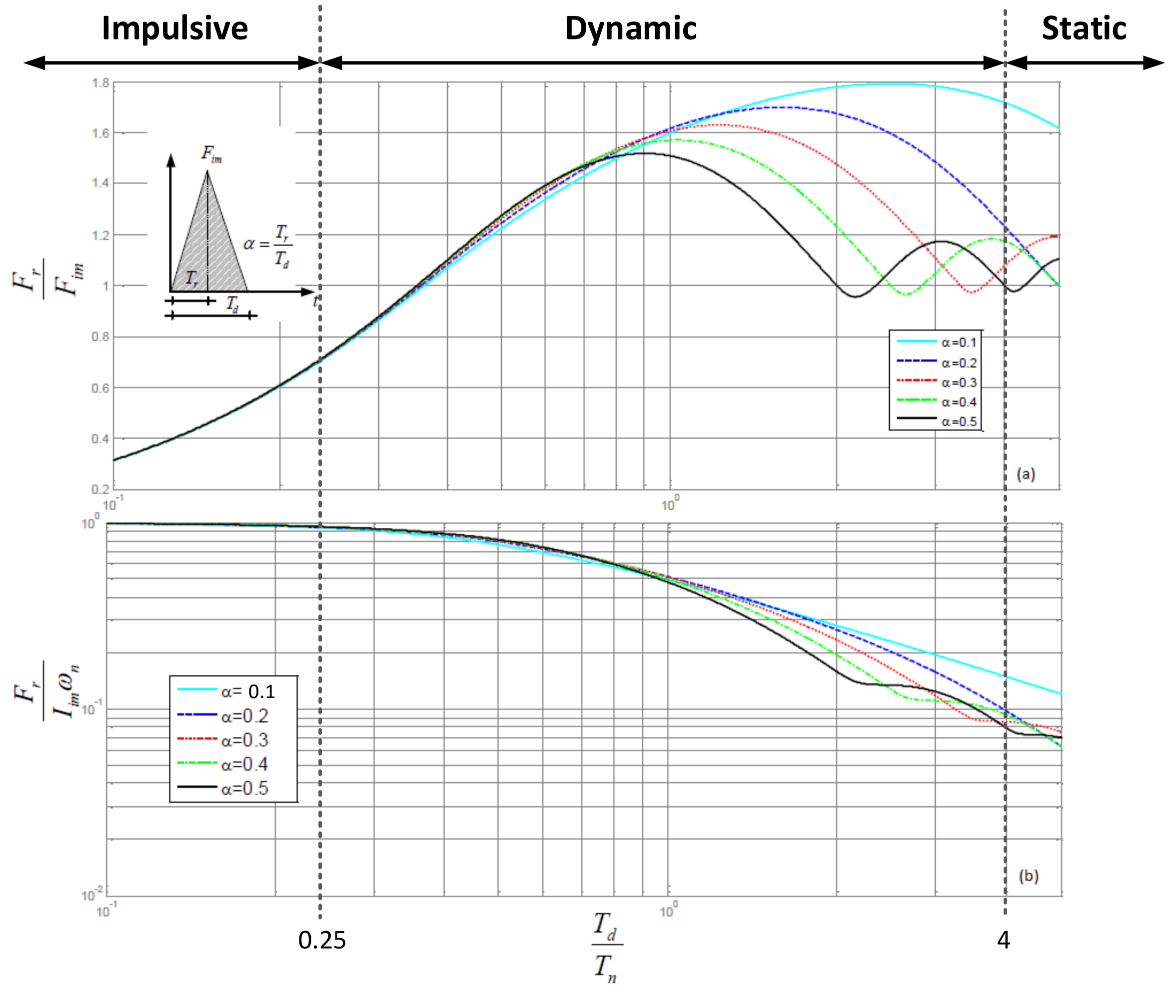

Fig. 4: Response function for a linear SDOF system subject to triangular pulse having a total duration time of T_d. Top: based on maximum impact force, referred to Eq 1. Bottom: based on impact impulse, referred to Eq 2.

4. Experimental setup and test program

Hydraulic structures like sluice gates, lock gates often contain vertical steel gates. Sometimes, this gate has an overhanging beam in the front. Kolkman and Jongeling (2007) remarked that for such kind of vertical structure with a specific overhanging type beam, impulsive wave impacts are expected to occur based on laboratory and field measurements and observations. Thus, measurements of such a structure are used as a test case for the envisaged approach. A structural model to represent a sluice gate with an overhanging beam of the Afsluitdijk in the Netherlands was schematized by using a vertical wall with a beam. A series of physical model experiments were undertaken by Deltares to determine the design wave impact load on such a structure. Fig. 5 shows the schematic of the physical model test of wave impacts on Afsluitdijk sluice gate. The model tests are performed on a geometric scale of 1:16. To convert the model results to prototype values, some scale rules will be considered. The main rule of scale for a proper representation of the wave motion is that the ratio of the main driving forces in the model (gravity and inertia) are similar to those in the prototype. This starting point forms the basis of Froude's scaling law.

4.1. Wave flume

The tests were performed in the Scheldt Flume of Deltares. This flume has a length of 55 m, a width of 1 m, and a height of 1.2 m (model scale). Its second-order wave generator can generate regular (monochromatic) and irregular (random) waves. The wave generator is equipped with an active wave absorption system (ARC) to minimize reflection of waves.

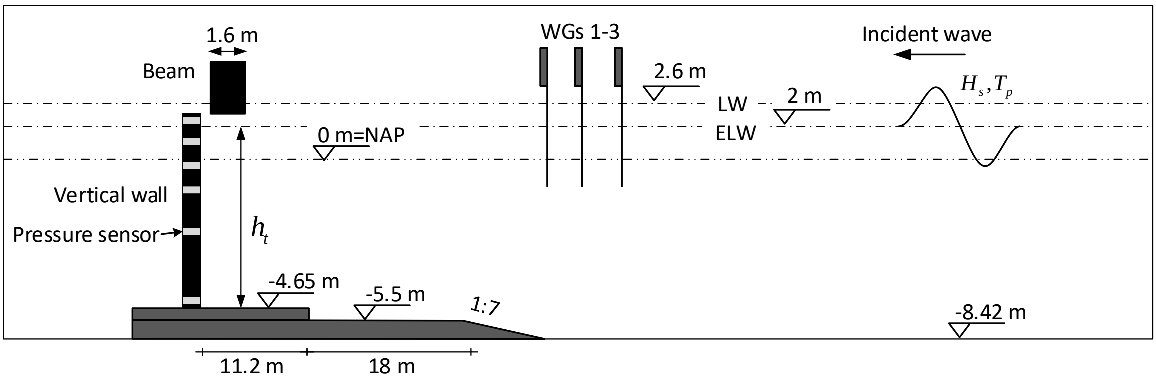

Fig. 5: Schematic sketch of wave flume and wave parameter definition in prototype scales. The wave height is 10000 year condition.

4.2. Instrumentation

The wave height is measured with an array of three wave gauges located at the toe of the foreshore (WGs 1-3 in Fig. 5). With an array of 3 wave height meters, Mansard and Funke (1980)'s method determines the incoming wave signal. From this the significant wave height H_s, and the wave period T_p are determined.

Six pressure sensors were mounted on the surface of the vertical wall with a sampling frequency at 4000 Hz. The natural frequency of the vertical wall with the horizontal overhang model is more than 100 Hz in model scale, so a frequency of more 25 Hz in reality. In the pressure signal no influence of vibration was seen at this frequency.

With a 2-megapixel color CCD high speed video camera, recordings were made throughout the test from the side of flume at 100 frames per second. With a second normal camera, images from other viewing angles of short sections of the test have also been made.

4.3. Test program

Impulsive impacts on the sluice gate were observed during the tests with low water levels (LW) and extreme low water levels (ELW). The incident waves are confined, resulting in impulsive impacts at the corner of the sluice gate and the overhanging. Test program is shown in Table 2.

Table 2: The test program (prototype scale).

Test series	Water depth h_t [m]	Wave height H_s [m]	Wave period T_p [s]
T1-LW	7.25	2.09	4.88
T1-ELW	6.65	2.09	4.85
T2-LW	7.25	1.76	4.97
T2-ELW	6.65	1.74	4.97

5. Results

5.1. Impulsive loads on the wall

5.1.1. Observations

Two types of wave impacts on the wall were observed. One is the most impulsive impact ($F_{max}/F_{qs+} > 2.5$) and the other one is a moderate impact ($F_{max}/F_{qs+} < 2.5$), based on the classification defined by Kortenhaus and Oumeraci (1998). For the moderate impact, the incident wave does not break in front of the wall. This non-breaking wave forms a standing wave. The upward wave directly impacts on the overhang beam, which gives extra horizontal force on the wall, see Fig 6. The term 'wave 1' is used to denote this upward impact in this paper. For the impulsive impact , the incident wave starts to break directly on the

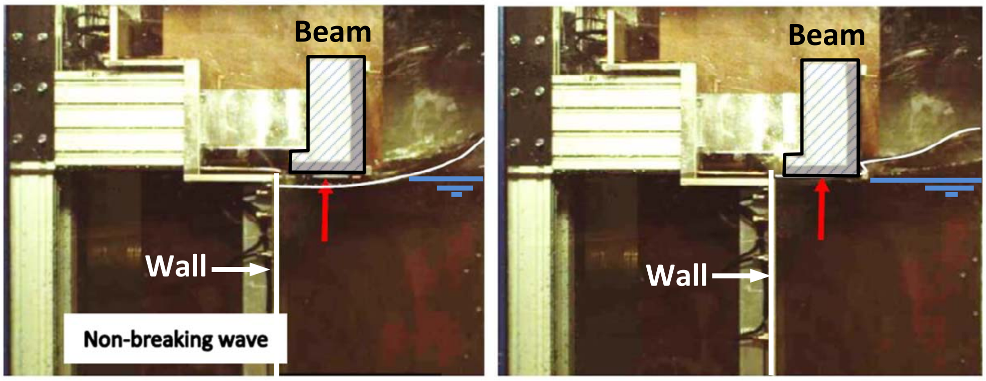

Fig. 6: Wave 1: Moderate wave impact which is measured in test T1-LW at 5865 s. The white line indicates the water surface, blue lines are the still water level, and the red arrows show the direction of the water surface.

structure, as shown in Fig 7. The term 'wave 2' is used to express the waves. The upper panel of Fig 7 shows the incident wave approaching the model, and the bottom panel provides the impact moment of this wave. When the incident wave approaches the wall, the water surface below the overhang moves rapidly upwards (like ① in Fig 7). The main part of the wave above the still water surface is impacting on overhang. The water below the overhang is confined and pushed onto the wall (like ② in Fig. 7). Therefore, the impact of wave 2 consists two processes: initial vertical impact on the beam, and following a horizontal impact on the wall. This horizontal impact gives a strong impact on the wall.

Table 3: Wave impact types based on the classification defined by Kortenhaus and Oumeraci (1998)

Wave impacts [%]	T1-LW	T1-ELW	T2-LW	T2-ELW
No impact	0	0	0	0
Moderate impact	25.7	34.9	42.3	37.3
Impulsive impact	74.3	65.1	57.7	62.7

The types of wave impacts of the four tests were distinguished as shown in Table 3. The influence of water level and wave heights are shown below.

- Water level

  Two water levels were tested in this study. The term 'LW' means low water level which is slight above the bottom of the beam, whereas the term 'ELW' means extreme low water level, which is slightly below the bottom of the beam. Comparing the tests T1-LW and T1-ELW (with large wave height), it can be seen that there are more impulsive impact events in T1-LW than that in T1-ELW. But the force of the wave impacts of test T1-ELW is larger than that in T1-LW. This is because the lower water provide enough space (below the bottom of the beam) for large waves to impact and be confined at the

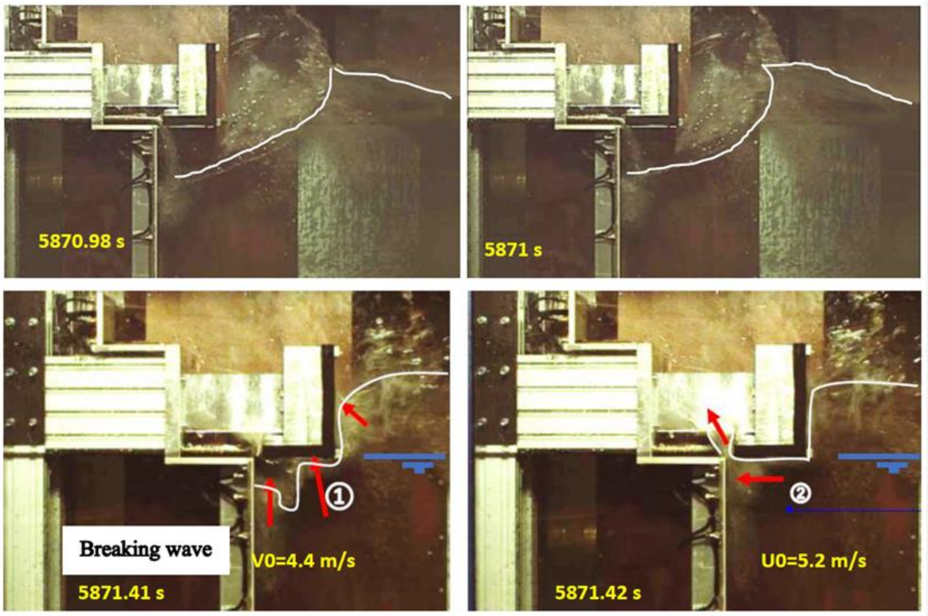

Fig. 7: Wave 2: the largest wave impact moment which is measured in the test T1-LW. The top panel left: 0.57 s before impact on the gate, top panel right:0.41 s before impact on the gate; bottom panel left: 10 ms before the impact, bottom panel right: impact. The white line indicates the water surface, the red arrows the velocity of the water surface.

corner between the wall and the beam. Especially for T1-LW, large waves just impact on the beam, but not the wall. While for the tests T2-LW and T2-ELW (with small wave height), the observations are opposite. ELW gives more violent impacts than LW.

- Wave height

  Comparing the tests T1-LW and T2-LW, it can be seen that there are more impulsive impact events in T1-LW with large wave height than that in T2-LW with small wave height. But for the tests T1-ELW and T2-ELW with much lower water level than T1-LW and T2-LW, the differences between the two types of impacts are not obvious.

Thus, a low water level combined with a large incident wave leads to the most unfavorable condition.

5.1.2. Splitting impulsive and quasi-steady force components

An impulse model is developed based on designing a low-pass filter to split the impulsive and quasi-steady force components. It is realized by analyzing the evolution of energy spectrum of wave impacts and water surface elevations near the structure in time-frequency domain. The filter is based on continuous 1-D wavelet transform (CWT) and inverse continuous 1-D wavelet transform (ICWT) by using the functions from MATLAB 2016. The CWT is used to get the wavelet spectrum (as shown in Fig. 8a and b), and

ICWT is used to get the filtered force signal in time domain (as shown in Fig. 8*c*). The default Morse (3,60) wavelet and default scales in obtaining the CWT are used.

Fig. 8a and Fig. 8b show examples of the CWT spectrum for water surface elevations measured at WG6 and the time series of four-wave impacts obtained by integration of the six pressure sensors of test T1-LW. The colour bar of each spectrum indicates the range of the wavelet energy. In Fig. 8a and b, two energy bands are observed at around 0.1-0.35 Hz and 0.35-0.65 Hz during the whole test respectively. In Fig. 8b, four energy peaks are clearly located at the higher frequency parts. By comparing both CWT spectrums, the consistency of the occurrence of the energy bands are believed caused by different components of wave motions. Therefore, quasi-steady force and impulsive force can be split at 0.65 Hz in frequency domain. Fig. 8c presents the original measured time series of the four wave impact forces (two moderate and two impulsive impacts) corresponding to the CWT spectrum of Fig. 8b. The filtered time series of quasi-steady wave forces at 0.35 Hz and 0.65 Hz are plotted together. It can be seen that the filtered quasi-steady forces obtained by using low-pass filters at 0.35 Hz (red dashed line) and 0.65 Hz (black dashed dot line) match each other well for the two moderate impact waves. It indicates that the choice of using a low-pass filter with cut-off frequency at 0.65 Hz to split quasi-steady forces caused by slowly wave motion is reasonable. As for the two impulsive impacts, the peak quasi-steady forces with 0.65 Hz are a bit higher than those with 0.35 Hz. This gives insights that the steepness of the wave increases before the impact, which is in line with the impulsive impact mechanisms, as described by Kortenhaus and Oumeraci (1998).

5.1.3. Equivalent impact duration

After the step of splitting, the time series of the quasi-steady and the impulsive components of wave impacts are obtained. Due to the irregularity (and oscillation) of the time series of the impulsive force, it is difficult to determine the impact duration of the impulse T_d and the further dynamic response. A symmetrical triangular pulse is used to schematize the impact impulse with I_{im} and the peak impulsive force F_{im} constant. Then the equivalent impact duration $T_{d,e}$ can be calculated as: $2I_{im}/F_{im}$.

Fig. 9 shows the plot of impact duration versus the impact impulse for test T1-EWL. The red circle marker indicates the impact duration obtained directly from the impulsive force signal, and black right triangular marker indicates the equivalent impact duration. It can be seen that most of the duration is overlapped when T_d is less than 0.2 s especially for those between 0.08 and 0.18 s, where impact impulses have high values. In this study, we only focused on the impulsive type of impact which has a short duration. Thus, the calculated equivalent impact duration is reasonable to represent the impact duration of impulsive impacts. Thus, in the following of this paper, the impact duration T_d means the equivalent impact duration.

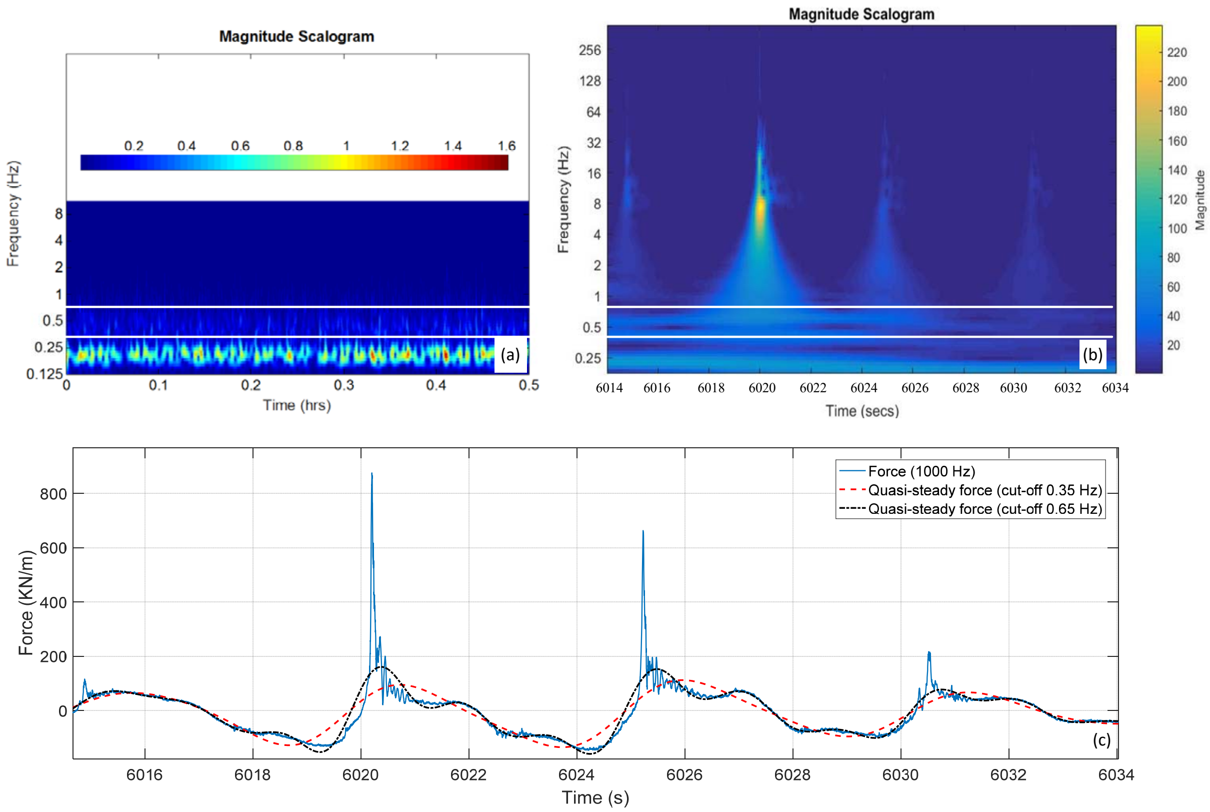

Fig. 8: Example of wavelet transformation based filter to separate quasi-steady and impulsive impact components. (a) CWT spectrum for the water surface elevations obtained by wave gauge at WG6 of the whole test T1-LW. (b) CWT spectrum for the time series of wave impacts (from 6014 s till 6034 s) obtained by integration of the six pressure sensors of test T1-LW. (c) Examples of the wave impacts time series (from 6014 s till 6034 s) without filtering (blue line) is shown together with a quasi-steady force obtained by using ICWT with a low pass filter at a cut-off frequency 0.35 Hz (red dash line) and the quasi-steady force from the same original force time series, but at a cut-off frequency 0.65 Hz (black dot dash line).

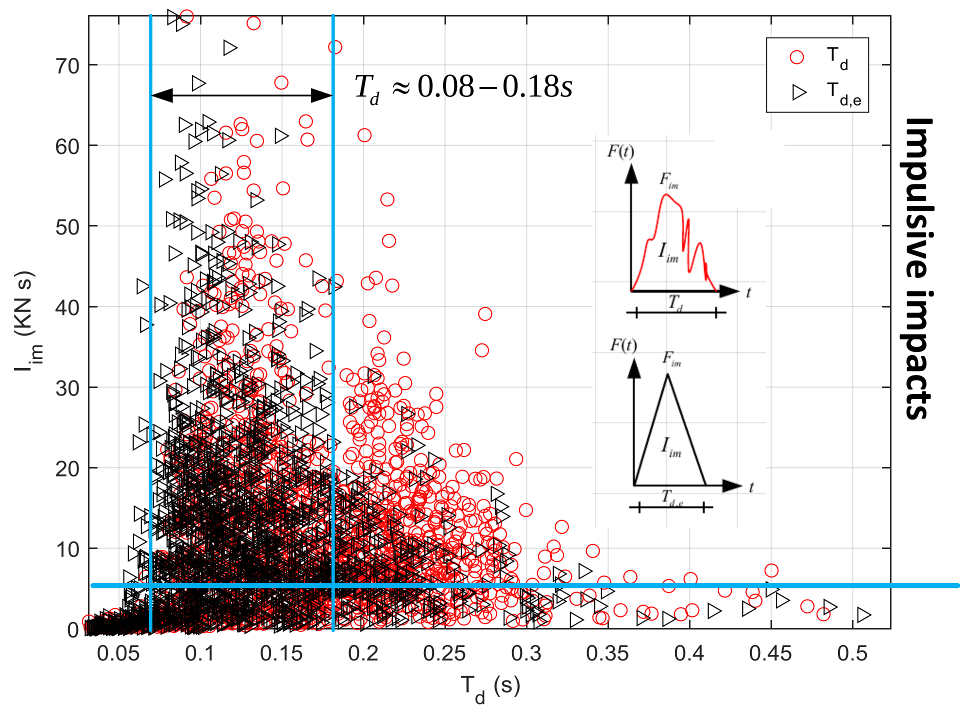

Fig. 9: Comparison of impact duration and equivalent impact duration.

5.2. Reaction forces and reconstructed reaction forces

5.2.1. Procedure for simulated reaction force in prototype

The total reaction force $F_{tot,r}$ of the vertical wall in prototype to the wave impact need to be calculated, since it may be amplified due to dynamic effect. The real reaction force can be simulated by using SDOF model and indicated as $F_{\mathtt{SDOF}}$ in the following part of the paper.

5.2.2. Evaluation of the envisaged method

The proposed method for determining $F_{tot,r}$ is based on the assumption that structural reactions can be reconstructed by the reactions of the quasi-steady (F_{qs+}) and the impulsive components (F_{im}) of the wave impact force. Since F_{qs+} is assumed within the static loading domain of the structure (see Fig. 4), the reaction force to the quasi-steady impact ($F_{qs+,r}$) would equal to the F_{qs+}. Whereas the reaction force to the impulsive impact ($F_{im,r}$) may be amplified due to the dynamic effect.

In order to evaluate the assumption of the reconstruction, $F_{im,r}$ is simulated by the same SDOF model aforementioned, but using the impulsive component of the measured force signal. Thus the simulated real reaction force to the impulsive component of the wave impact $F_{\mathtt{im,r,SDOF}}$ is determined. $F_{tot,r}$ can be reconstructed by using the following Eq. 3:

$$F_{tot,r} = F_{qs+} + F_{\mathtt{im,r,SDOF}}. \tag{3}$$

Four SDOF models with varied natural frequencies at 2 Hz, 10 Hz, 20 Hz and 50 Hz are selected. By changing the characteristics of the SDOF model, the dynamic effect of the SDOF to the wave impact are different. The simulated prototype total reaction forces of these structure $F_{\mathtt{tot,r,SDOF}}$ are compared with $F_{tot,r}$ by using Eq. 3, as shown in Fig. 10. The red line indicates the 1:1 reference line. The results show that there is a good agreement between $F_{tot,r}$ using the proposed splitting method in this study and $F_{\mathtt{SDOF}}$. Thus, the proposed method with splitting the two components of the wave impacts is applicable.

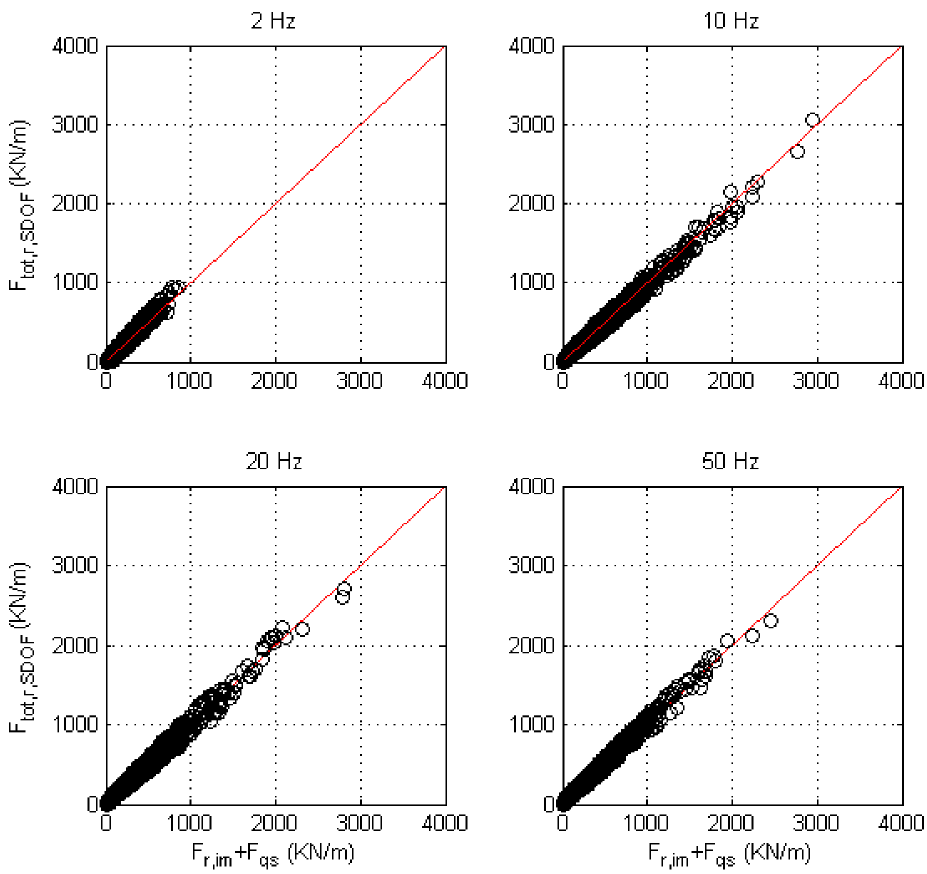

Fig. 10: Responses of four SDOF models with 2 Hz, 10 Hz, 20 Hz and 50 Hz respectively to wave impacts versus the calculated reaction force by using Eq. 3.

Furthermore, the aim of this study is to estimate $F_{tot,r}$ by using the impact impulse I_{im}. When the impulsive impact component is separated from the measured wave impact force signal, I_{im}, T_d, and F_{im} are determined. $\mathrm{DLF_M}$ is used to estimate the dynamic response of the structure to the impulsive wave impact.

The impulsive impact is simplified as a symmetrical triangular pulse ($\alpha = 0.5$), which is characterized by the equivalent impact duration $T_{d,e}$, I_{im}, and F_{im}. Thus, by using $\mathrm{DLF_M}$, the total reaction force $F_{tot,r}$ is expressed as Eq.4:

$$F_{tot,r} = F_{qs+} + I_{im} \cdot \omega_n \cdot \mathrm{DLF_M}. \tag{4}$$

where $\mathrm{DLF_M}$ is defined in Eq. 2. This expression is only using I_{im} and equivalent duration $T_{d,e}$. The value of $\mathrm{DLF_M}$ can be determined from the graph as shown in Fig. 4*b*. In order to compare the work performance of Eq.4, $F_{tot,r}$ is also calculated with a more conventional approach by using DLF, as shown in Eq. 5:

$$F_{tot,r} = F_{qs+} + \mathrm{DLF} \cdot F_{im} \tag{5}$$

where DLF is the dynamic load factor (Eq. 1) using this expression, F_{im} and $T_{d,e}$ need to be known. The value of DLF can be determined from the graph as shown in Fig. 4*a*. In a common practice, a most conservative value 1.52 is used for DLF to consider the dynamic effect with an assumption of the force shape as a symmetrical triangular ($\alpha = 0.5$). Thus Eq. 5 can be simplified as:

$$F_{tot,r} = F_{qs+} + 1.52 F_{im}. \tag{6}$$

The performance of Eq. 4 and Eq. 6 are compared and discussed in the later section.

5.3. Statistical analysis of impact impulse and quasi-steady force

A storm contains many individual waves. To obtain a certain design load due to impulsive impacts, extreme value analysis is conducted. The time series of the wave force on the vertical structure were obtained from the physical model tests. Individual and independent F_{qs+} and I_{im} for all four tests were identified from the time series of the split forces.

5.3.1. Statistical analysis of impact impulse

There is a positive correlation between wave forces and I_{im}. Fig. 11a shows such a linear trend between F_{im} and F_{qs+} and I_{im} of each impact of test T1-ELW respectively. It can approximately be said that large impulsive force F_{im} has a large impact impulse, the same as F_{qs+}. Therefore, the thresholds of I_{im} and wave forces are defined based on the ratio of the impulsive impacts of all impacts (see Table 3) to distinguish the impulsive wave impacts. For example, for test T1-LW, the impulsive impact takes up 74.3% of total impacts. Thus, a threshold for impact impulse I_{tr} used for extreme value analysis is set as the top 74.3% quantile of the total impact impulses I_{im}, the same method is used for F_{qs+}.

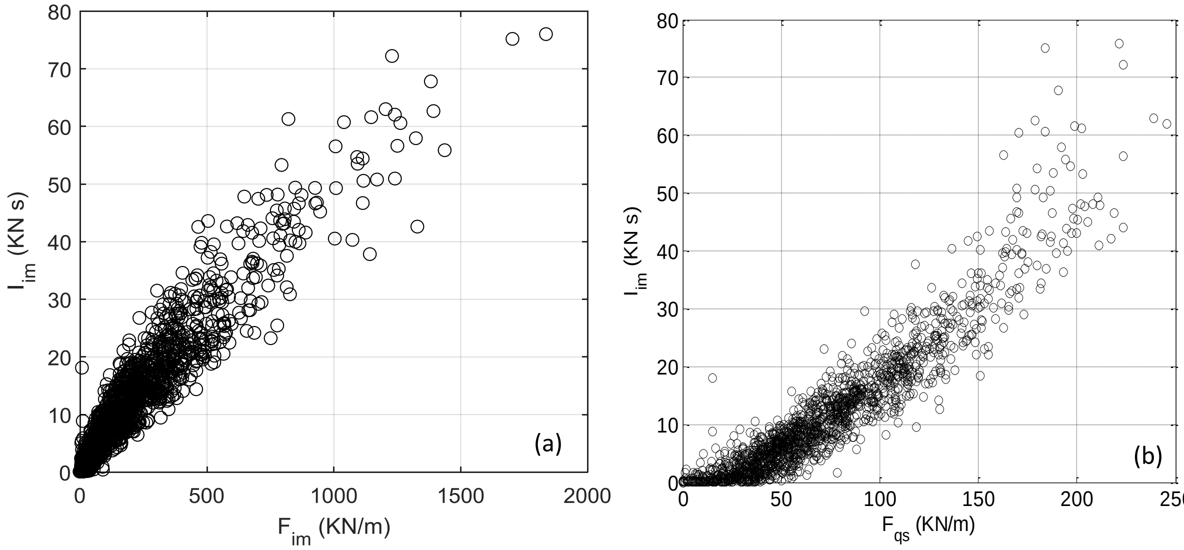

Fig. 11: Impulsive impact forces versus impact impulse of test T1-ELW.

Dimensionless impact impulse $I^* = \frac{I_{im}}{\rho H^2 U}$ is used in the further analysis, where H and U are length scale and velocity scale respectively. The length scale defined herein as $H = H_s$ and the velocity scale as $U = \sqrt{g\,(h_t + 0.5 H_s)}$. Fig. 12 shows the exceedance probability of each I^* induced by impulsive wave impacts of each test. y-axis indicates the exceedance probability of I^*_i above the threshold I^*_{tr} and the x-axis indicates the relative value of I^*_i. It can be seen that the individual impact impulse from the tests with the same water levels (e.g., T1-LW and T2-LW) follow the same trend.

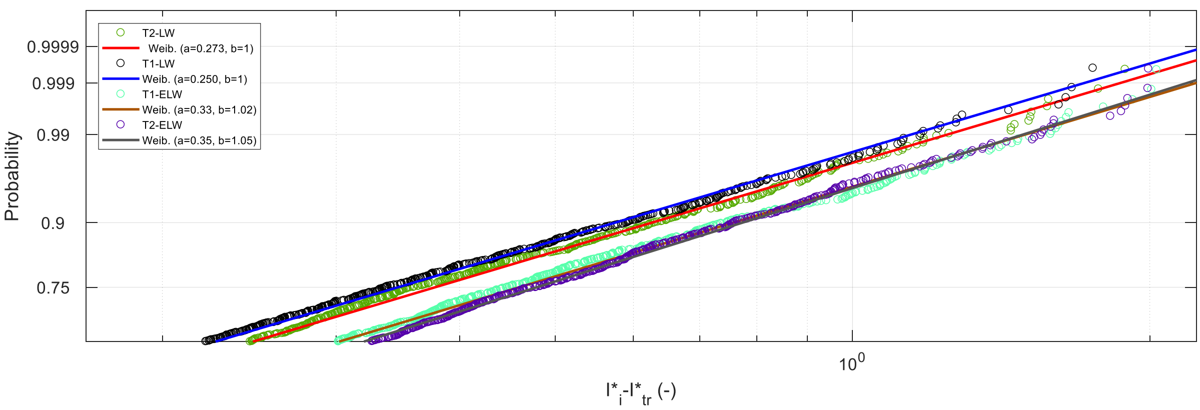

Fig. 12: Weibull distribution fit for the four tests. Markers indicate the individual impact impulses above the threshold, and the lines indicate the best-fit. a and b indicates the scale and shape parameters of the best fit Weibull distribution.

5.3.2. *Statistical analysis of quasi-steady force*

Fig. 11b shows a linear trend between the peak quasi-steady force and its impact impulse of each impact of test T1-ELW. This shows that waves that lead to large quasi-steady forces also lead to large impact impulses. Therefore, the threshold of the quasi-steady force $F_{qs,tr}$ is based on the ratio of the impulsive impacts of all impacts (see Table 3). For example, for test T1-LW, the impulsive impact takes up 74.3% of the total impacts. Thus, a threshold for quasi-steady force used for extreme value analysis is set as the top 74.3% quantile of the total quasi-steady forces. Dimensionless quasi-steady force $F^*_{qs+} = \frac{F_{qs+}}{\rho g H_s^2}$ is used in the further analysis, where H_s is the significant wave height.

Fig. 13 shows the exceedance probability of each dimensionless quasi-steady force induced by impulsive wave impacts of each test. The y-axis indicates the exceedance probability of $F^*_{qs+,i}$ above the threshold $F^*_{qs+,tr}$ and the x-axis indicates the relative value of the dimensionless impact impulse. It can be seen that most of the quasi-steady force of the four tests follow the same trend, only the tails of the distributions are separated.

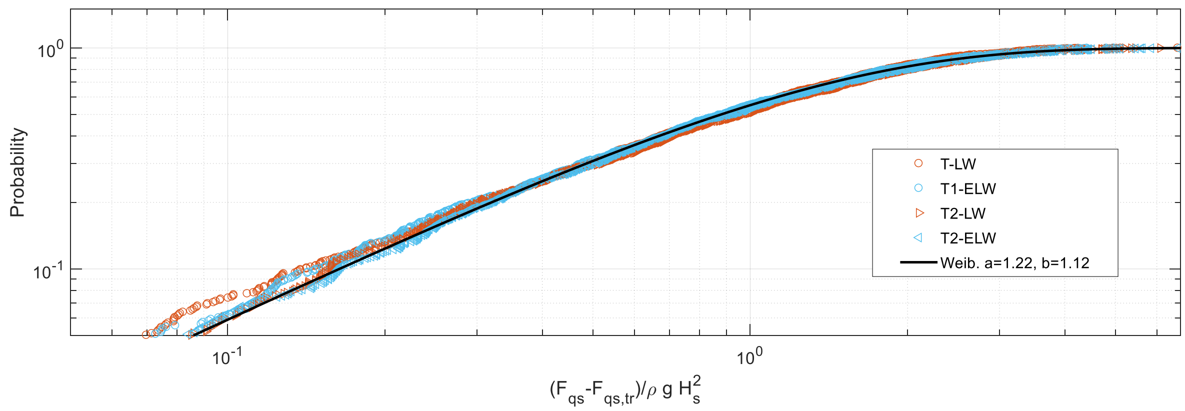

Fig. 13: Weibull distribution fit for the four tests. a and b indicates the scale and shape parameters of the best fit Weibull distribution.

5.3.3. *Evaluation of total reaction forces by statistical analysis*

In this section, the distributions of impact impulses and quasi-steady forces for the impulsive wave impacts are used. The exceedance level of F_{qs+} and I_{im} depends on the degree of correlation between these two parameters. The correlation is large, as can be seen in Fig. 10b.

A design load with a 0.1% exceedance probability ($X_{0.1\%}$) is selected for testing the performance of the proposed approach in this study. X indicates the impact event e.g., $X = I_{im}$ or $X = F_{qs+}$. The impact duration is fixed to the most "unfavorable" duration 0.09 s, which is determined from Fig. 9. The term "unfavorable" is the one with leading to the highest impulsive impact. Four structures (SDOF models) are considered, with natural frequencies of 2 Hz, 10 Hz, 20 Hz and 50 Hz. The impulsive impact $I_{im,0.1\%}$ with impact duration 0.09 s will fall in the impulsive ($T_d/T_n < 0.25$), dynamic ($0.25 < T_d/T_n < 4$) and static ($T_d/T_n > 4$) loading domains of the considered structures.

The result of T1-ELW is shown in Table 4 as an example. F_s is the total wave force at 0.1% exceedance level directly measured from the test, without consideration of the structural response. DLF_M is the dynamic load factor expressed in a form of impulse, which is determined from Fig. 4b. Herein a rising time ratio $\alpha = 0.5$ is chosen for DLF_M. F_{DLF_M} is obtained by using the method developed in this study (Eq. 4), in which $I_{im,0.1\%}$ is obtained from the curve fitting. $F_{qs+,0.1\%}$ is obtained from the best curve fitting. F_{DLF} is calculated by Eq. 6, where F_{im} is using the difference of F_s and $F_{qs+,0.1\%}$. $F_{M,r}$ is the minimum value of F_{DLF_M} and F_{DLF}, which is used to represent the reaction force based on the model tests. $F_{\texttt{SDOF}}$ is the reaction forces from SDOF models which are used to represent the 'real' reaction force of different structures.

For structures with natural frequencies at 10 Hz, 20 Hz and 50 Hz, the total wave force F_s is less than F_{DLF_M}. The structure with 10 Hz leads to the highest reaction force F_{DLF_M}. Thus, if using F_s determined from the measurement as the design load, the 'real' dynamic force is underestimated for the structures with natural frequencies of 10 Hz, 20 Hz and 50 Hz, or too conservative for the structure with natural frequency of 2 Hz. If using F_{DLF} as the design reaction force, the 'real' dynamic force is conservative for most of the four structures although the dynamic effect of the structure has been considered.

Table 4: A design reaction force with a 0.1% exceedance probability with wave force peak F_s 1844 KN/m, which consists of the impact duration $T_d = 0.09$ s with a rising time ratio $\alpha = 0.5$.

Load Domains	stru.	T_d/T_n	DLF_M	I_{im}	F_{qs+}	F_{DLF_M}	F_{DLF}	$F_{M,r}$	$F_{\texttt{SDOF}}$
Impulsive	2 Hz	0.18	0.9736	74.6	228.5	1141	2684	1141	954.7
Dynamic	10 Hz	0.9	0.5366	74.6	228.5	2742	2684	2684	2627
Dynamic	20 Hz	1.8	0.196	74.6	228.5	2065	2684	2065	2565
Static	50 Hz	4.5	0.0729	74.6	228.5	1935	2684	1935	2108

Comparing the values of $F_{M,r}$ and $F_{\texttt{SDOF}}$ in different loading domains, $F_{M,r}$ is less than $F_{\texttt{SDOF}}$ for the case $T_d/T_n = 1.8$ and $T_d/T_n = 4.5$. The reason of this underestimation of the reaction forces may be led by the assumption of the shape of impulse: the impulse is a symmetry triangle with rising time ratio $\alpha = 0.5$. From the response spectrum shown in Fig. 4, it can be concluded that the DLF varies when $T_d/T_n > 0.9$ for different impulse shapes, whereas for the case $T_d/T_n < 0.9$, there is no such influence. Thus, the assumptions of impulse with a symmetric shape with rising time ratio α equaling to 0.5 may be not applicable when $T_d/T_n > 0.9$, which will lead to the underestimation of the reaction force. Fig. 14 shows the trend of the calculated reaction force with considering the effect of the rising time ratio. It can be seen that the assumption of a symmetric impulse shape is not applicable when the impulse falls into the end region of dynamic and static loading domains of the structure. A rising time ratio with 0.4 is suggested for these cases.

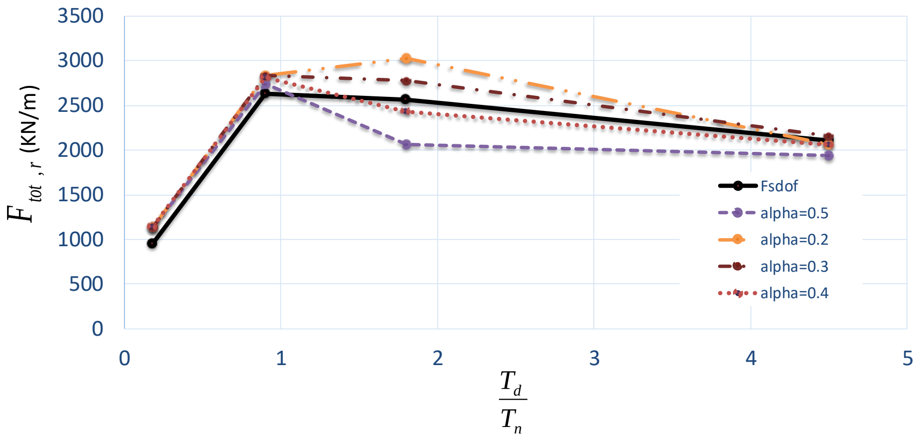

Fig. 14: Effect of α on the reaction forces of test T1-ELw.

6. Discussion

In this paper, an envisaged method to estimate the design reaction force is presented with including certain aspects that influence the wave impact load, like determining the exceedance probability of a certain load, incorporating the flexibility of the structure.

There are other aspects of using the concept of impact impulse for designing a structure that can be incorporated in this method, like determining the spatial distribution of the wave loads since the extreme value of the impact impulse (e.g., $I_{im0.1\%}$) has been determined. Good agreement is found between the measured pressure-impulse and the results of the Cooker and Peregrine (1995)'s model. This part of analysis is presented in Appendix A. The results indicate that the pressure impulse model can be used to derive the spatial distribution of the pressure impulse from an extreme impulse obtained from an EVA for a vertical wall with an overhang.

The impulse is assumed as a systematic triangle shape with a rising time ratio 0.5 which excites the structure. In general, this assumption works well when the impulse falls into the impulsive and part of the dynamic loading domains when $T_d/T_n < 1$. But for the latter half of dynamic and static loading domain, both the shape and duration of the impulse are important. Choosing a symmetric triangle shape impulse to represent the real impact may lead to underestimation of the reaction force. For this case, an asymmetric triangle shape with a rising time ratio of 0.4 is recommended. It should be noted that the dynamic response of the structure due to quasi-steady force is not considered. This situation may occur when the considered structure has an extremely long natural vibration period. Thus, the proposed method is not applicable for this case. It is suggested to take the minimum value of F_{DLF_M} by using the proposed impulse expression and the traditional F_{DLF} by using a DLF 1.52 as the design reaction force. The latter one always provides conservative values which may overestimate the real dynamic force.

Using impulse as the input to design a structure is not a new concept. Using force peak and impulse are most widely used design methods in structural engineering field. For example, in USACE (1957) to design of structures to resist the effects of atomic weapons, it is clearly stated that using force and impulse (based on energy approach) to design structure to resist impacts are both good. Using the force as input is good to analysis the structure behavior, while using the impulse as input is good to design a structure. The novity of the proposed approach in the paper is to describe a method of using the impulse of wave impact to design a hydraulic structure. More efforts are still needed to improve the statistical model (e.g., develop an impulse distribution formula which parameters can be empirically determined by wave climate and structure geometry characteristics) and structure model (the typology of the structure) in the future .

In this study, four tests with two wave conditions and two water levels were statistically analyzed. For impact impulse, the exponential distribution (Weibull distribution with shape parameter $b = 1$) was found to provide the best fit. For quasi-steady forces, the Weibull distribution fits the four tests data well. The scale parameter is expected to be empirically described by the incident wave conditions in front of the structure. However, the proposed distribution is limited to the current test range. In an extension of this research, the authors propose that empirical parameterized distributions of impact impulses and quasi-steady forces will be obtained from more measurements and CFD calculations with a varied range of wave characteristics and structural geometries. This part of analysis is presented in Appendix B.

The exact shape of the pressure peak and the impact duration have a large scatter (e.g., Hofland et al., 2010) and are prone to scale effects (e.g., Ramkema, 1978). Hence, the impact duration and the shape of the impact impulse can be altered based on empirical evidence. It might be that the impact is in the dynamical domain of the structure. Then the most adverse duration might be chosen as a conservative design approach, or a probabilistic approach can be used to estimate the joint probability of a certain extreme force. But for a detailed characterization the impact loads, a joint distribution between the impact impulses and the impact duration, or the quasi-steady forces and the impact duration are suggested for the future research.

7. Conclusion

The wave impact load on a vertical wall with overhang is analyzed using the impact-related impulse (integral of impact force over the impact duration) as the primary load variable instead of the peak impact force. A wavelet-based method to split the quasi-steady and impulsive components of the impact force is presented. Extreme value distributions are derived for both the impact-related impulse and the pulsating (quasi-steady) forces. Statistical values of impact-related impulse and quasi-steady force can be recombined to predict the total load for a certain probability of occurrence, that can be used to determine the dynamical response of the structure. Small scale model tests of wave impacts on a vertical wall with an overhanging beam were used to try out this method. The results show that the proposed method can provide a good estimation of the reaction force when the structure is excited by an impulsive wave impact.

Acknowledgments

This research was supported by Rijkswaterstaat RWT31120028.

Appendix A. Pressure-impulse theory and application

According to Lamb (1932), an impulsive impact occurs when a fluid surface suddenly hits a rigid surface. When the impact duration is very short, the pressure impulse field in the fluid can be calculated, by only knowing the changes in velocities around the edges of the fluid domain (i.e. impact velocities). Based on this fact, Cooker and Peregrine (1990, 1995) proposed a pressure impulse (P) theory to predict the impact impulse of the pressure peak. The pressure impulse is defined as the time integral of the pressure over the impact duration $P = \int_{t_b}^{t_a} p dt$, as shown in Fig A.15a. By assuming a very short duration of the impact, both gravity and the nonlinear terms involving a spatial derivative of velocity terms can be neglected (Cooker and Peregrine, 1990, 1995; Wood, 1997). Based on the foregoing assumption, the considered impact is limited to the impulsive peak. Thus, the hydrostatic pressure from the slow water motion (e.g., red dashed quasi-steady force in Fig 2) needs to be removed from the whole pressure time history (Oumeraci et al., 2001). The pressure impulse can be approximately calculated by solving the Laplace equation, $\nabla^2 P \approx 0$, with known boundary conditions, as shown in Fig A.15b.

An example of using the pressure-impulse theory to get the spatial pressure impulse distribution along the vertical wall is provided in Fig. A.16a. The input horizontal velocity (U_0) and vertical velocity (V_0) were extracted from the velocity field of each wave through PIV analysis.

Good agreement is found between the measured pressure-impulse P and the results of the Cooker and Peregrine (1995)'s model, using the measured values of U_0, V_0, and μH. The results indicate that the pressure impulse model can be used to derive the spatial distribution of the pressure impulse from an extreme impulse obtained from an EVA for a vertical wall with an overhang.

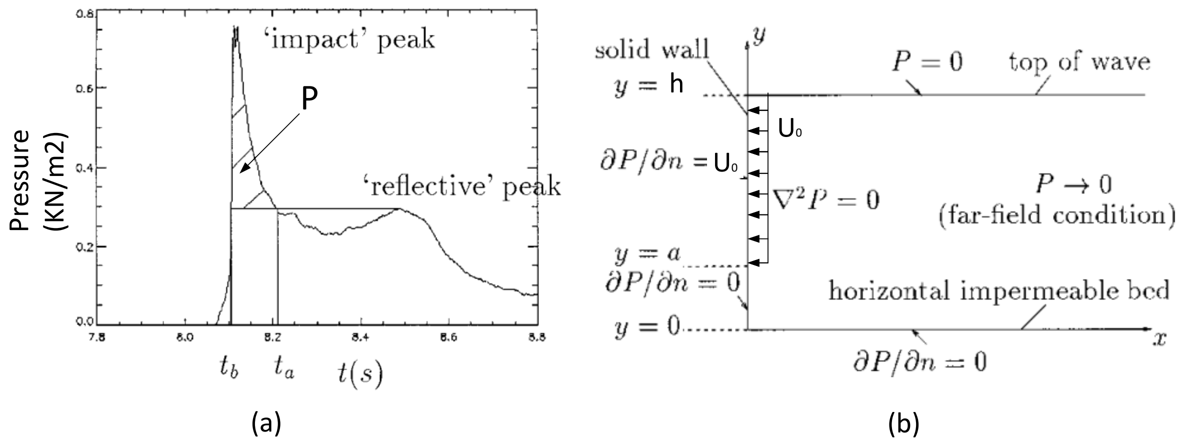

Fig. A.15: (a) typical pressure-time history for impact on wall (b) boundary conditions on pressure impulse for impact on wall for a 2D vertical case with a wave impacting the wall on the left with a velocity of U_0, and over a height of (h-a) (adapted from Wood et al., 2000).

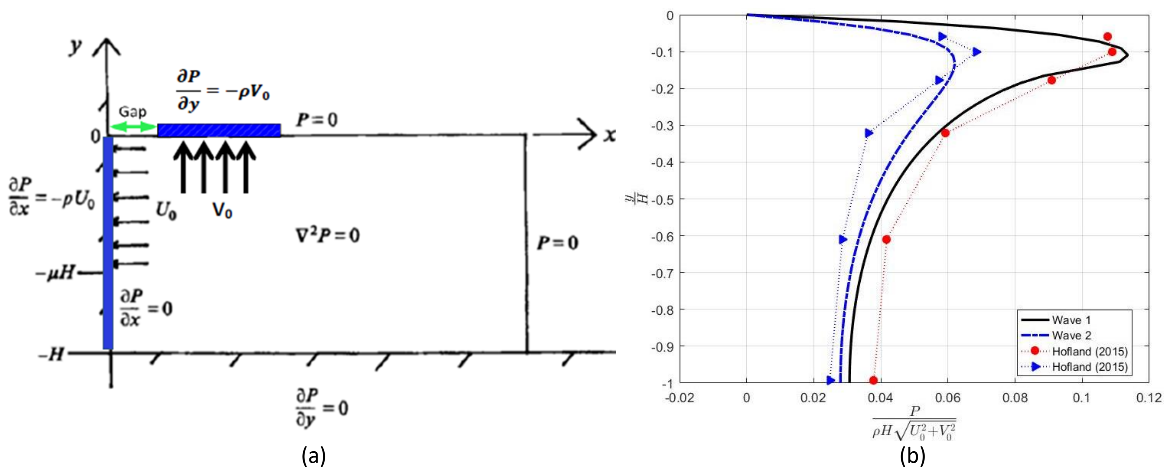

Fig. A.16: (a) Modified boundary condition for the vertical wall with an overhang beam; (b) the calculated pressure-impulse distribution by using modified Cooker and Peregrine (1995)'s pressure impulse theory with boundary conditions of 2 types of waves (see section 5.1.1)

Appendix B. Statistical model and its applied results

Weibull distribution is verified as the best distribution to characterize the impact impulse, expressed as below:

$$P_{I^*}\left(I_i^* - I_{tr}^* \geq I_*\right) = \exp\left[-\left(\frac{I_i^* - I_{tr}^*}{a}\right)^b\right] \tag{B.1}$$

where a and b indicates the scale and shape parameters of the distribution. The fitting results are also shown in Fig. 12 and Table A1. It can be seen that the shape parameters of the four tests are close to 1. Thus, as a special case of Weibull distribution, exponential distribution (with shape parameter equals to 1) is used to simply represent the distribution of impact impulse. For the tests with the same water level, the scale parameters are nearly the same. Thus, a hypothesis is made that the scale parameter of the impact impulse distribution may be a function of water depth. Then the m_{th} I_m can be calculated as follow:

$$I_m = I_{tr} - a\ln\left(\frac{P_m}{P_{im}}\right) \tag{B.2}$$

with P_m the exceedance probability of the m_{th} largest impulsive impact force peak of the total impacts N_{im} with expressing as $m/(N_{im}+1)$, whereas P_{im} is the occurrence of the impulsive wave impact of the total impacts with expressing as $N_{im,i}/(N_{im}+1)$. In this study, incoming wave number N_w is simply determined as the number of generated waves in each test.

Applying the Weibull distribution provided the best fit. Table A2 shows the fitting results. As the scale and shape parameters for all tests are quite close, $a = 1.22$ and $b = 1.12$ are used to characterize the quasi-steady force in this study. Fig. 13 also shows the fitting results of Weibull distribution by using $a = 1.22$ and $b = 1.12$ (black line). The final probability distribution for quasi-steady force is expressed as below:

$$P\left(F_{qs+,i}^* - F_{qs+,tr}^* \geq F_{qs+}^*\right) = \exp\left[-\left(\frac{F_{qs+,i}^* - F_{qs+,tr}^*}{1.22}\right)^{1.12}\right] \tag{B.3}$$

The proposed distributions for impulse and quasi-steady force are limited to the current test range. In an extension of this research, the authors propose that empirical parametric distributions of impact impulses and quasi-steady forces will be obtained from more model tests and CFD calculations with a varied range of wave characteristics and structural geometries.

Table A1: Summary of the results for Weibull distribution fitting

Test series	N_w	N_{im}	$N_{im,i}$	I^*_{tr}	Scale a	Shape b
T1-LW	2000	1583	1176	0.057	0.25	1
T1-ELW	2000	1635	1064	0.159	0.33	1.02
T2-LW	2000	1891	1091	0.097	0.27	1
T2-ELW	2000	1795	1125	0.174	0.35	1.05

Table A2: Summary of the results for weibull distribution fitting for quasi-steady force

Test series	N_w	N_{im}	$N_{im,i}$	$F^*_{qs+,tr}$	Scale a	Shape b
T1-LW	2000	1583	1176	0.47	1.18	1.15
T1-ELW	2000	1635	1064	1.24	1.2	1.12
T2-LW	2000	1891	1091	1.04	1.27	1.10
T2-ELW	2000	1795	1125	1.42	1.24	1.11

Appendix C. List of Symbols

F_{qs+}	quasi-steady force
$F_{qs+,r}$	the reaction force to the quasi-steady impact
$F_{qs+,0.1\%}$	quasi-steady force with exceedance probability of 0.1%
$F^*_{qs+,tr}$	threshold of dimensionless quasi-steady force
$F^*_{qs+,i}$	dimensionless quasi-steady force of i event
F_s	wave force peak from the measurement
F_{im}	impulsive force
F_{max}	total force peak
F_r	reaction force
$F_{tot,r}$	total reaction force reconstructed by the reactions of F_{qs+} and F_{im}
$F_{tot,r,0.1\%}$	$F_{tot,r}$ with exceedance probability of 0.1%
$F_{0.1\%}$	force peak with exceedance probability of 0.1%
$F_{r,0.1\%}$	reaction force with exceedance probability of 0.1%
$F_{im,r}$	reaction force to the impulsive impact
$F_{im,r,0.1\%}$	reaction force to the impulsive impact with exceedance probability of 0.1%
F_{SDOF}	the real reaction force can be simulated by using SDOF model
$F_{im,r,\mathrm{SDOF}}$	the simulated real reaction force to the impulsive component of the wave impact
$F_{tot,r,\mathrm{SDOF}}$	the simulated prototype total reaction forces of these structure
I_{im}	impact impulse
$I_{im,0.1\%}$	impact impulse with exceedance probability of 0.1%
I^*	dimensionless impact impulse
I^*_i	dimensionless impact impulse i event
I_{tr}	threshold of impact impulse
T_d	impact duration
$T_{d,e}$	equivalent impact duration
T_n	natural period of the structure
α	rising time ratio
ω_n	natural angular frequency of the structure
H	length scale of pressure-impulse theory
U	velocity scale of pressure-impulse theory
H_s	Significant wave height
T_p	Significant wave period
h_t	water depth in front of the structure
X	impact event

Reference

Bagnold, R.A., 1939. Interim report on wave-pressure research. Technical Report. Institution of Civil Engineeris.

Bullock, G., Crawford, A., Hewson, P., Walkden, M., Bird, P., 2001. The influence of air and scale on wave impact pressures. Coastal Engineering 42, 291–312. doi:10.1016/S0378-3839(00)00065-X.

Castellino, M., Sammarco, P. , Romano,A., Martinelli, L. , Ruol, P. , Franco, L. ,De Girolamo, P. 2018. Large impulsive forces on recurved parapets under non-breaking waves. A numerical study. Coastal Engineering 136, 1–15. doi:10.1016/j.coastaleng.2018.01.012.

Chan, E.S., Melville, W.K., 1988. Deep-Water Plunging Wave Pressures on a Vertical Plane Wall. Proceedings of the Royal Society A: Mathematical, Physical and Engineering Sciences 417, 95–131. doi:10.1098/rspa.1988.0053.

Chen, X., Hofland, B., Uijttewaal, W., 2016. Maximum overtopping forces on a dike-mounted wall with a shallow foreshore. Coastal Engineering 116, 89–102.

Cooker, M., Peregrine, D., 1990. A model for breaking wave impact pressures. Coastal Engineering Proceedings 1.

Cooker, M.J., Peregrine, D.H., 1995. Pressure-impulse theory for liquid impact problems. Journal of Fluid Mechanics 297, 193.

Cuomo, G., Allsop, W., Bruce, T., Pearson, J., 2010a. Breaking wave loads at vertical seawalls and breakwaters. Coastal Engineering 57, 424–439. doi:10.1016/j.coastaleng.2009.11.005.

Cuomo, G., Allsop, W., Takahashi, S., 2010b. Scaling wave impact pressures on vertical walls. Coastal Engineering 57, 604–609.

Farge, M., 1992. Wavelet transforms and their applications to turbulence. Annual review of fluid mechanics 24, 395–458.

Hofland, B., Kaminski, M., Wolters, G., 2010. Large scale wave impacts on a vertical wall. Coastal Engineering Proceedings 1, 15.

Humar, J.L., 2002. Dynamics of structures. A.A. Balkema Publishers.

Kirkgoz, M., Mengi, Y., 1986. Dynamic response of caisson plate to wave impact. Journal of Waterway, Port, Coastal, and Ocean Engineering 112 2,pp. 284–295,

Kisacik, D., Troch, P., Van Bogaert, P., 2012. Experimental study of violent wave impact on a vertical structure with an overhanging horizontal cantilever slab. Ocean Engineering 49, 1–15. doi:10.1016/j.oceaneng.2012.04.010.

Kolkman, P., Jongeling, T., 2007. Dynamic behaviour of hydraulic structures. WL— Delft Hydraulics publication .

Kortenhaus, A., Oumeraci, H., 1998. Classification of wave loading on monolithic coastal structures. Coastal Engineering Proceedings

Lamb, H., 1932. Hydrodynamics. Dover publications.

Lamberti, Alberto, Martinelli, Luca, 1998. Prototype measurements of the dynamic response of caisson breakwaters. Coastal Engineering Proceedings

Losada, MA., Martin, FL, Medina, R, 1995. Wave kinematics and dynamics in front of reflective structures. Wave Forces on Inclined and Vertical Wall Structures. Task Committee on Forces on Inclined and Vertical Wall Structures, pp. 282–310. ASCE.

Mansard, E.P., Funke, E., 1980. The measurement of incident and reflected spectra using a least squares method, in: Coastal Engineering 1980, pp. 154–172.

Massel, S.R., 2001. Wavelet analysis for processing of ocean surface wave records. Ocean Engineering 28, 957–987.

Md Noar, N., 2012. Wave impacts on rectangular structures. Ph.D. thesis. Brunel University, School of Information Systems, Computing and Mathematics.

Md Noar, N.A.Z., Greenhow, M., 2015. Wave impacts on structures with rectangular geometries: Part 1. Seawalls. Applied Ocean Research 53, 132–141.

Misiti, M., Misiti, Y.,Oppenheim, G.,Poggi, JM, 2004. Matlab Wavelet Toolbox User's Guide. Version 3. MathWorks

Nagai, S., 1973. Wave Forces on Structures . Advances in Hydroscience 9 pp. 253–324. Academic Press, New York.

Nørgaard, J.r.Q.H., Andersen, T.L., 2014. Distribution of wave loads for design of crown walls in deep and shallow water. Coastal Engineering Proceedings 1, 47.

Oumeraci, H., Klammer, P., Partenscky, H., 1993. Classification of breaking wave loads on vertical structures. Journal of Waterway, Port, Coastal, and Ocean Engineering 119, 381–397.

Oumeraci, H., Kortenhaus, A., Allsop, W., de Groot, M., Crouch, R., Vrijling, H., Voortman, H., 2001. Probabilistic Design Tools for Vertical Breakwaters.

Ramkema, C, 1978. A model law for wave impacts on coastal structures, in: Coastal Engineering Proceedings 1978, pp. 2308–2327.

Sainflou, G., 1928. Essai sur les digues maritimes verticales. Annales de ponts et chaussées, vol 98, tome II, 1928 (4) pp 5-48 .

Takahashi, S., Tsuda, M., Suzuki, K., Shimosako, K., 1998. Experimental and fem simulation of the dynamic response of a caisson wall against breaking wave impulsive pressures. Coastal Engineering Proceedings 1

Tieleman, O.C., Tsouvalas,A., Hofland, B, Peng, Y., Jonkman, S.N 2018. A three dimensional semi-analytical model for the prediction of gate vibrations immersed in fluid, submitted to: Marine Structures

Wood, D., Peregrine, D., 1997. Wave impact beneath a horizontal surface, in: Coastal Engineering 1996, pp. 2573–2583.

Wood, D.J., 1997. Pressure-impulse impact problems and plunging wave jet impact. Ph.D. thesis. University of Bristol.

Wood, D.J., Peregrine, D.H., Bruce, T., 2000. Wave impact on a wall using pressure-impulse theory. i: trapped air. Journal of waterway, port, coastal, and ocean engineering 126, 182–190.

United States. Army. Corps of Engineers, 1957. Engineering and design: design of structures to resist the effects of atomic weapons: principles of dynamic and design. Dept. of the Army, Office of the Chief of Engineers.